Supplementary Information for Ultrafast magnetization enhancement in metallic multilayers driven by superdiffusive spin current

Dennis Rudolf,[1*] Chan La-O-Vorakiat,[2*] Marco Battiato,[3*] Roman Adam,[1] Justin M. Shaw,[4] Emrah Turgut,[2] Pablo Maldonado,[3] Stefan Mathias,[2,5] Patrik Grychtol,[1,2] Hans T. Nembach,[4] Thomas J. Silva,[4] Martin Aeschlimann,[5] Henry C. Kapteyn,[2] Margaret M. Murnane,[2] Claus M. Schneider[1] and Peter M. Oppeneer[3]

[1]*Peter Grünberg Institut PGI-6 & JARA-FIT, Research Centre Jülich, 52425 Jülich, Germany*
[2]*Department of Physics and JILA, University of Colorado and NIST, Boulder, CO, USA*
[3]*Department of Physics and Astronomy, Uppsala University, SE-75120 Uppsala, Sweden*
[4]*Electromagnetics Division, National Institute of Standards and Technology, Boulder, CO, USA*
[5]*University of Kaiserslautern and Research Center OPTIMAS, 67663 Kaiserslautern, Germany*

Corresponding author: r.adam@fz-juelich.de

SUPPLEMENTARY FIGURES

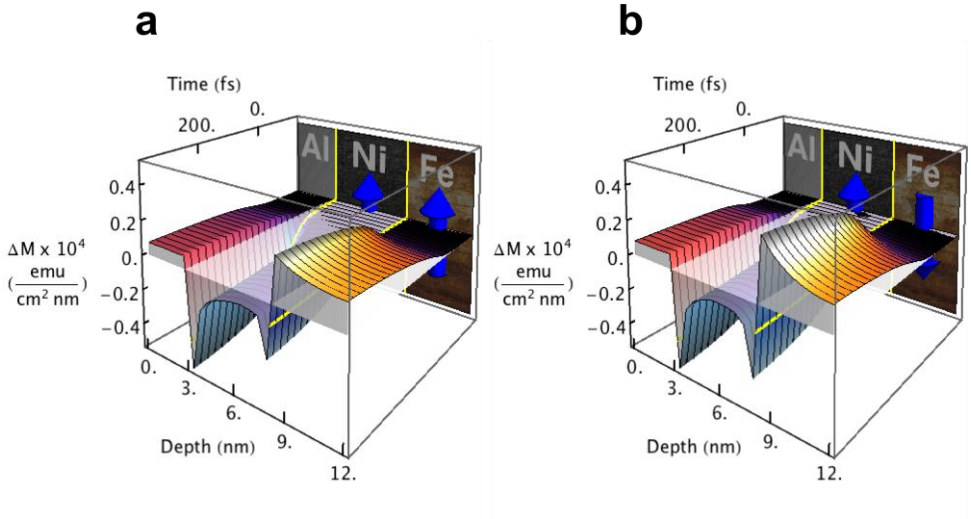

Supplementary Figure S1| Evolution of the trilayer magnetization in space and time. The magnetization change ΔM compared to the case of thermal equilibrium in a trilayer consisting of Al, Ni and Fe layers is displayed for parallel **(a)** and antiparallel **(b)** magnetization alignment within the first 500 fs after laser excitation along the depth profile of the layers. The Ni spin-majority electrons move by superdiffusion predominantly from the interface region into the Fe and Al layers, thus decreasing the Ni magnetization.

[*] These authors contributed equally to this work.

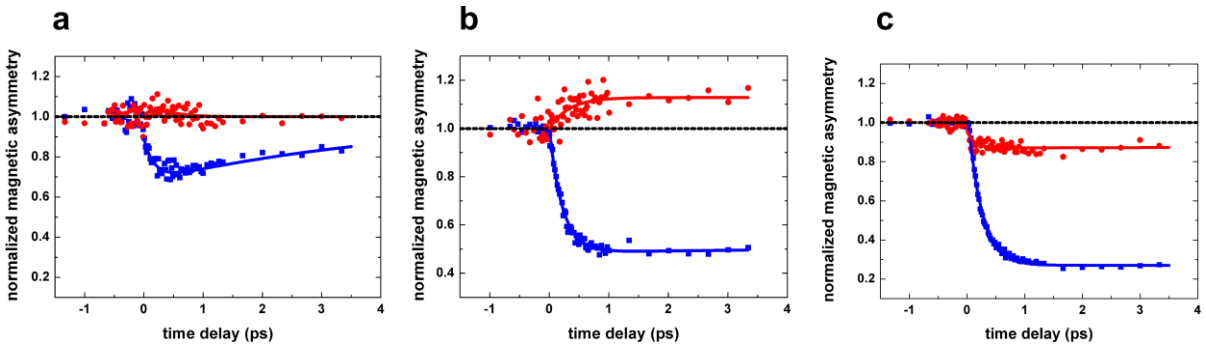

Supplementary Figure S2| Fluence-dependent time- and layer- resolved magnetization. The effect of the superdiffusive spin-transfer current on the magnetization dynamics of the Fe layer can only be observed if other demagnetization channels are small in comparison. By measuring the laser fluence dependence of the spin dynamics for *parallel* magnetization alignment of the Ni and Fe layers, we identified the optimal conditions for observing a magnetization enhancement due to superdiffusive spin currents reaching the Fe layer. Experimentally, for laser pump fluences of 1.3 mJ/cm^2, there is a weak transient enhancement of the Fe magnetization for parallel Fe/Ni magnetization alignment **(a)**. When the laser fluence is increased to 2.0 mJ/cm^2, we observe the strongest *magnetization enhancement* **(b)**. For an even higher fluence of 2.7 mJ/cm^2, we observe the onset of an additional demagnetization channel in Fe, which acts in the opposite direction to the superdiffusive spin-transfer from the Ni and the magnetization in the Fe layer displays ultrafast *demagnetization* **(c)**. Such behavior is consistent with the expectation that the generation of superdiffusive spin currents in the top Al/Ni layers saturates at the laser pump fluence between 2.0 and 2.7 mJ/cm^2.

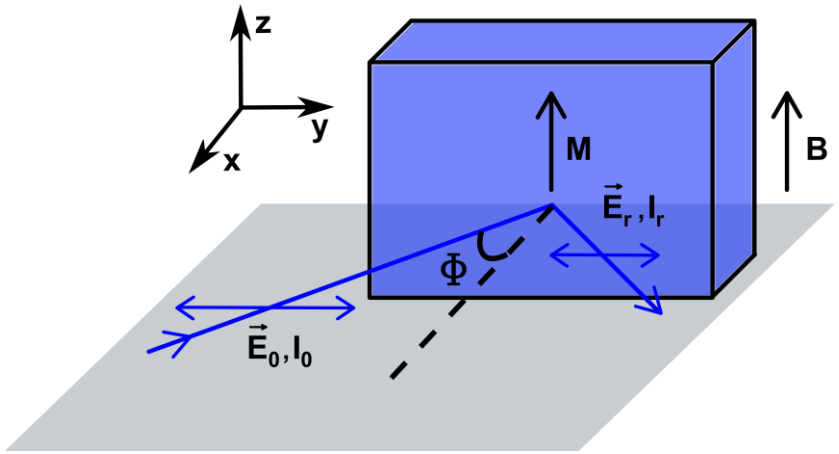

Supplementary Figure S3| Geometry of the transverse magneto-optical Kerr effect (T-MOKE). The amplitude of the incident electric field E_0 linearly polarized in the x-y-plane penetrating the sample at angle Φ is changed by the magnitude and the direction of the sample magnetization M pointing in the z-direction perpendicular to the plane of incidence. Thus, the reflected electric field amplitude E_r and the intensity I_r depend on M.

SUPPLEMENTARY TABLE

	τ_m (in fs)		τ_r (in ps)	
	↑↑	↑↓	↑↑	↑↓
Ni(5 nm)/Ru(1.5 nm)/Fe(4 nm)	219 ±19	136±24	> 200	15±10
Ni(5 nm)/Ru(1 nm)/Fe(4 nm)	208±33		22±17	

Supplementary Table S1| Demagnetization (τ_m) and remagnetization (τ_r) times. The relevant values were obtained from time-resolved T-MOKE magnetic asymmetry measurements integrating over the Ni 3p absorption edge (around 66 eV) for parallel and antiparallel magnetization orientation of the Ni and Fe layers. A phenomenological exponential equation, Supplementary Equation S2, is used to extract the time parameters.

SUPPLEMENTARY DISCUSSION

Superdiffusive spin transport theory was used to describe the dynamics of ultrafast, non-equilibrium, laser-excited electrons[12,13] in magnetic multilayers. The governing equation Eq. (2) (see Methods in the main text) provides a geometrically exact kinematic description of the excited electron transport on femtosecond timescales. It therefore models accurately the laser-generated spin-polarized electron transport, which is essential since excited electron lifetimes in ferromagnetic *3d*-metals like Ni and Fe are of the order of a few tens of femtoseconds, while the mean-free-paths are on the order of the thickness of the layered structure. Therefore, commonly adopted transport approximations such as ballistic or standard diffusion models cannot be used.

Superdiffusion-driven magnetization dynamics can be viewed as arising from two main effects. One important contribution to the magnetization dynamics originates from the interface between two different materials, as pointed out in the previous publications [12,13], where the transport properties change abruptly, thereby resulting in regions of spin accumulation. A second contribution is due to volumetric spin depletion in an optically excited layer.

The theoretical demagnetization times τ_M can be obtained by fitting the computed element-specific $\Delta M(t)$ curves in Figure 5 of the main text with Supplementary Equation S2. This gives τ_M = 148±10 fs for both parallel and antiparallel alignment of Ni with respect to the Fe layers. We predict essentially the same values for the Fe demagnetization time in an antiparallel geometry with respect to Ni, and for the Fe anomalous magnetization increase in a parallel geometry. Comparable demagnetization times are also extracted from the experimental data (Supplementary Table S1).

In Supplementary Figures S1a and S1b, we report the computed position- and time-dependent changes in the magnetization, i.e. $\Delta M(z,t)$, of the Al/Ni/Fe layers, calculated as the superposition of the transport of spin up and down electrons (see Supplementary Methods). The z-coordinate is defined as perpendicular to the layers, starting at the Al surface. The values for the static magnetization used for Ni and Fe are 0.38 10^{-4} emu/(cm^2 nm) and 1.39 10^{-4} emu/(cm^2 nm), respectively. The resulting magnetization change profiles look similar for the parallel and antiparallel alignment of Ni and Fe films. They are not similar in fact, but appear to be because the transport properties of non-equilibrium electrons in Fe are poorer and have a lower spin asymmetry than those in Ni.

Let us consider in more detail the laser-induced spin transport. First, superdiffusive electrons excited in the Al enter the Ni layer. Upon entering the Ni layer, the two spin channels experience very different transport properties. Spin-majority electrons are unimpeded as they traverse the Ni layer, eventually reaching the Fe layer. Conversely, spin-minority electrons accumulate within the first half nm in the Ni layer. Second, electrons that are directly excited in the Ni layer exhibit a different behavior. Non-equilibrium spin-majority electrons in Ni can easily superdiffuse out of the layer, transferring spin angular momentum into the neighboring layers, thereby causing an induced magnetization change in Fe and Al (Supplementary Figure S1). Spin-minority electrons excited in the Ni layer are immobilized by scattering in the region where they

are created, to a first approximation. Third, electrons are also excited in the Fe layer, with the amount of excited electrons depending on the laser fluence reaching the Fe. However, the excited hot electrons in Fe do not exhibit the same good transport properties as those of Ni or Al; the spin transport asymmetry for Fe is weaker, and both spin channels are less amenable to superdiffusion. Hence, with the aim of having an intuitive understanding of the superdiffusion in this layered structure, we can approximately assume that spin-majority and -minority excited electrons are essentially trapped once they enter the Fe. This further explains the small difference in ΔM for Fe shown in Supplementary Figures S1a and S1b.

One must also consider that the electron transport does not evolve in a purely ballistic way but rather the electrons undergo inelastic electron-electron scatterings in the layers. In addition, they can be reflected at the surfaces and interfaces. Screened electrons escaping from the Ni layer become mainly trapped in the Fe layer. Even screened electrons that superdiffuse first into the Al layer can be reflected at the Al-vacuum interface and travel back towards the Fe layer, because of the good transport properties of Al. We emphasize that the calculated results shown in Supplementary Figure S1 have been obtained by solving the superdiffusive equation with the proper transport quantities – the purpose of the simplified explanation above only serves to assist in an intuitive analysis of the data.

Fluence-dependent time- and layer-resolved magnetization measurements, further confirming the above model, are discussed in some detail in Supplementary Figure S2.

SUPPLEMENTARY METHODS

In our experiment, the magnetic signal is measured in the transverse magneto-optical Kerr effect (T-MOKE) geometry (Supplementary Figure S3). The reflected amplitude of linear *p*-polarized light depends on the magnetization component of the sample oriented perpendicular to the plane of incidence. Defining the magnetic asymmetry *A* by Eq.(1) of the main text, it is possible to relate *A* to the dielectric properties of the sample. Assuming ε_{xx} to be the diagonal element of the dielectric tensor, ε_{xy} the off-diagonal element, ε_0 the vacuum dielectric permittivity and Φ the angle of incidence, the expression for *A* for a single-element film becomes[36]

$$A = \mathrm{Re}\left(\frac{2\varepsilon_0 \varepsilon_{xy} \sin(2\Phi)}{\varepsilon_{xx}^2 \cos^2(\Phi) - \varepsilon_0 \varepsilon_{xx} + \varepsilon_0^2 \sin^2(\Phi)} \right). \qquad \text{(S1)}$$

At the atomic absorption edges, the off-diagonal element of the dielectric tensor ε_{xy} is resonantly enhanced and therefore, the magnetic asymmetry is increased from less than one percent in the visible spectral range[37], up to tens of percent[23]. The increase of ε_{xy} over its analogue in the visible spectral range is due to the large spin-orbit and exchange splitting of the *3p* shallow core states[38]. The magnetic asymmetry signal becomes additionally amplified at the pseudo-Brewster angle[23]. In our experiment, we generate a spectrum of high harmonics with photon energies spanning the XUV region. (Harmonics up to the absorption edge of Al (72.6 eV [http://henke.lbl.gov/]) are used to probe the sample). This enables us to perform spectroscopic measurements at the Fe and Ni *3p* absorption edges (52.7 eV and 66 eV, respectively), probing the magnetic response of both elements simultaneously. The experimental asymmetry data can be reproduced by simulations based on the Maxwell equations with appropriate boundary conditions[39,40]. The time-resolved magnetic asymmetry was fit to a double exponential function

$$A(t) = 1 - \Delta A\left[1 - \exp\left(-(t - t_0)/\tau_m\right)\right]\exp\left(-(t - t_0)/\tau_r\right), \qquad \text{(S2)}$$

adopted from [41], where ΔA denotes the quenching amplitude of the magnetization, t_0 the offset from the time zero, and τ_m and τ_r are the de- and remagnetization times. We analyzed the time-resolved magnetic asymmetry data by integrating over the *3p* absorption edge of Ni and Fe and normalizing the magnetic asymmetry to values obtained prior to laser excitation. The demagnetization (τ_m) and remagnetization (τ_r) times extracted from time-resolved T-MOKE measurements and fit using Supplementary Eq. S2 are shown in Supplementary Table S1.

SUPPLEMENTARY REFERENCES

36. Oppeneer, P. M. Magneto-optical Kerr spectra in Buschow, K. H. J. (ed.*)* Handbook of magnetic materials **13**, Elsevier, 229–422 (2001).

37. Afonso, C., Lagunas, A., Briones, F. & Girón, S. Magneto-optic Kerr effect in amorphous Fe_xSi_{1-x}. *Journal of Magnetism and Magnetic Materials* **15**, 833–834 (1980).

38. Valencia, S., Kleibert, A., Gaupp, A., Rusz, J., Legut, D., Bansmann, J., Gudat, W. & Oppeneer, P.M. Quadratic x-ray magneto-optical effect upon reflection in near-normal incidence configuration at the M edges of 3d transition metals. *Phys. Rev. Lett.* **104**, 187401 (2010).

39. Yeh, P. Optics of anisotropic layered media: a new 4 x 4 matrix algebra. *Surface Science* **96**, 41–53 (1980).

40. Visnovsky, S. Optics of magnetic multilayers. *Czechoslovak Journal of Physics* **41**, 663-693 (1991).

41. Guidoni, L., Beaurepaire, E. & Bigot, J.-Y. Magneto-optics in the ultrafast regime: thermalization of spin populations in ferromagnetic films. *Phys. Rev. Lett.* **89**, 017401 (2002).